Molecular Therapy
Nucleic Acids
Original Article

MSTN Attenuates Cardiac Hypertrophy through Inhibition of Excessive Cardiac Autophagy by Blocking AMPK/mTOR and miR-128/PPARγ/NF-κB

Hanping Qi,[1,2] Jing Ren,[1,2] Lina Ba,[1] Chao Song,[1] Qianhui Zhang,[1] Yonggang Cao,[1] Pilong Shi,[1] Bowen Fu,[1] Yongsheng Liu,[1] and Hongli Sun[1]

[1]Department of Pharmacology, Harbin Medical University-Daqing, Daqing, Heilongjiang 163319, China

Cardiac hypertrophy, a response of the heart to increased workload, is a major risk factor for heart failure. Myostatin (MSTN) is an inhibitor of myogenesis, regulating the number and size of skeletal myocytes. In recent years, cardiomyocyte autophagy also has been considered to be involved in controlling the hypertrophic response. However, less is known about the detailed mechanism of MSTN on cardiac hypertrophy via regulation of cardiomyocyte autophagy. In this study, we found that the deletion of MSTN potentiated abdominal aorta coarctation (AAC) and angiotensin II (Ang II)-induced pathological cardiac hypertrophy and cardiac autophagy; however, AAC and Ang II-induced cardiac hypertrophic phenotype and cardiac autophagy were dramatically diminished by MSTN *in vivo* and *in vitro*. Mechanistically, the anti-hypertrophic and anti-autophagic effects mediated by MSTN in response to pathological stimuli were associated with the direct inactivation of activated protein kinase (AMPK)/mammalian target of rapamycin (mTOR) and activation of the peroxisome proliferator-activated receptor gamma (PPARγ)/nuclear factor κB (NF-κB) signaling pathway. Additionally, miR-128 aggravated the progression of cardiac hypertrophy through suppressing its target PPARγ. Furthermore, MSTN downregulated miR-128 expression induced by AAC and Ang II. Taken together, MSTN significantly blunts pathological cardiac hypertrophy and dysfunction, at least in part, by inhibiting excessive cardiac autophagy via blocking AMPK/mTOR and miR-128/PPARγ/NF-κB signaling pathways.

INTRODUCTION

Cardiac hypertrophy has been regarded as individual myocyte growth in length and/or width, resulting in an increase in heart weight without an increase in the number of cardiomyocytes. Initially, such growth is an adaptive response to maintain cardiac pump function and decrease ventricular wall tension (compensatory hypertrophy). However, with prolonged cardiac hypertrophy, these changes become maladaptive and cause a significant increase in the risk for heart failure, leading to increased cardiovascular mortality.[1] There have been major advances in the identification of genes and signaling pathways involved in this disease process, but the overall complexity of hypertrophic remodeling suggests that additional regulatory mechanisms remain to be addressed.

Myostatin (MSTN), also known as growth and differentiation factor 8 (GDF-8), is a member of the secreted transforming growth factor β (TGF-β) superfamily of secreted growth factors and functions as a potent negative regulator of skeletal muscle mass.[2] This role is most dramatically demonstrated through inactivation of MSTN by engineered deletion and naturally occurring mutations leading to overt muscle hypertrophy in several species including mice and human beings.[3,4] Functionally, MSTN not only regulates the proliferation and differentiation of skeletal myogenesis, but also plays a decisive role in the regulation of metabolic processes. It has been observed that MSTN expression in adipose tissue is significantly higher in obese mice and obese patients than in normal mice and healthy humans.[5,6] In transgenic MSTN$^{-/-}$ mice, fat deposition was reduced compared with wild-type (WT) mice.[7]

Interestingly, in addition to the basic biological activities of MSTN in the regulation of muscle growth and metabolic processes, under different pathological conditions of the heart, MSTN is also strongly upregulated, arguing for a specific role in cardiac pathophysiology.[8,9] It has been reported that MSTN expression is increased in cardiomyocytes after cardiac infarction.[10] Recent studies also have in fact raised the intriguing possibility that MSTN may indeed influence cardiac muscle growth, suggesting that it may represent an effect related to the cardiac hypertrophy. George et al.[11] also have reported that MSTN is increased in heart failure patients. However, the underlying molecular mechanisms of MSTN in the regulation of cardiac muscle are still incompletely understood.

Autophagy is an evolutionarily conserved process for lysosomal degradation of proteins and other subcellular constituents.[12] Autophagy is initiated with formation of the double-membrane autophagosomes and subsequently degraded by lysosomes. Autophagy plays a pivotal role in removing aberrant or dysfunctional molecules and

Received 9 May 2019; accepted 2 December 2019;
https://doi.org/10.1016/j.omtn.2019.12.003.

[2]These authors contributed equally to this work.

Correspondence: Hongli Sun, Department of Pharmacology, Harbin Medical University-Daqing, Daqing, Heilongjiang 163319, China.
E-mail: hlsun2002@163.com

Table 1. Effects of MSTN on Echocardiographic Parameters in Pressure Overload-Induced Rat Hearts

	WT	WT+AAC	$MSTN^{-/-}$	$MSTN^{-/-}$+AAC
LVPWd (mm)	1.62 ± 0.04	2.82 ± 0.06*	1.65 ± 0.06	3.23 ± 0.21#
LVPWs (mm)	2.50 ± 0.07	3.45 ± 0.13*	2.47 ± 0.02	4.35 ± 0.12#
IVSd (mm)	1.65 ± 0.03	2.39 ± 0.04*	1.61 ± 0.02	3.35 ± 0.10#
IVSs (mm)	2.53 ± 0.07	3.49 ± 0.06*	2.47 ± 0.12	4.05 ± 0.13#
LVEF (%)	74 ± 2.04	56 ± 3.38*	75 ± 2.25	42 ± 2.16#
LVFS (%)	41 ± 1.87	36 ± 0.75*	40 ± 1.54	32 ± 1.03#

IVSd, diastolic interventricular septum thickness; IVSs, systolic interventricular septum thickness; LVEF, left ventricular ejection fraction; LVFS, left ventricular fractional shortening; LVPWd, diastolic left ventricular posterior wall depth; LVPWs, systolic left ventricular posterior wall thickness. Average data were represented by mean ± SD (n = 6). *$p < 0.05$ versus WT group; #$p < 0.05$ versus WT+AAC group.

intracellular organelles aggregates to maintain cellular function and protein quality. However, excessive levels of autophagy can result in the excessive degradation of organelles and eventually cell death.[13–15] Accumulated evidence has shown that exaggerated autophagic activity is associated with numerous diseases such as cancer, neurodegenerative disorders, and infectious diseases.[16–18] Especially, recent studies also illustrate that dysregulation of autophagy contributes to the pathogenesis of various forms of heart diseases, and its function is dose and environment dependent.[19–21] As we know, cardiac hypertrophy is characterized by increased cell size and enhanced protein synthesis, and is associated with the aggregation of misfolded proteins and damage of organelles, which can be cleared by a bulk degradation autophagic process.[22,23] A certain degree of autophagy activation is generally an adaptive response to eliminate damaged mitochondria and protein aggregates and compensate for energy loss, whereas exaggerated autophagic activity may foster cardiac hypertrophy development. However, the mechanisms regulating autophagy in cardiac hypertrophy are still poorly elucidated.

Accumulated evidence indicated that autophagy could be regulated by AMPK/mammalian target of rapamycin (mTOR) and nuclear factor κB (NF-κB) pathways. As we know, NF-κB is a protein complex that controls a large number of normal cellular and organismal processes and a downstream regulatory protein of peroxisome proliferator-activated receptor gamma (PPARγ). Moreover, PPARγ was most likely a potential target gene for the miR-128 predicted by miRanda software. Our preliminary experimental results demonstrated that MSTN could inhibit miR-128 expression. Simultaneously, AMPK could be suppressed by MSTN. Therefore, we hypothesize that there is a necessary link between MSTN and autophagy through the AMPK/mTOR and miR-128/PPARγ/NF-κB signaling pathways.

In this study, we created transgenic rat with deletion of MSTN to investigate the essential role of MSTN in cardiac hypertrophy and to explore the underlying mechanism. Moreover, we demonstrated that MSTN has a protective effect on cardiac hypertrophy by inhibiting exaggerated autophagic responses. This study suggested that MSTN might effectively rescue cardiac hypertrophy in rat, offering a possible therapeutic approach for cardiac hypertrophy.

RESULTS

MSTN$^{-/-}$ Rats Were More Susceptible to Pressure Overload

To examine whether endogenous MSTN contributed to cardiac hypertrophy, we generated global MSTN knockout (KO) rats. The absence of MSTN in the rat hearts was confirmed by western blot (Figure S1). The results of the echocardiographic examination showed that the parameters of left ventricular dimensions, such as diastolic interventricular septum thickness (IVSd), systolic interventricular septum thickness (IVSs), diastolic left ventricular posterior wall depth (LVPWd), and systolic left ventricular posterior wall thickness (LVPWs), were significantly increased between the rats from the WT+AAC (abdominal aorta coarctation) and $MSTN^{-/-}$+AAC groups at 10 weeks after AAC. The indices of cardiac systolic function, including left ventricular fractional shortening (LVFS) and left ventricular ejection fraction (LVEF), were significantly decreased between the rats from the WT+AAC and $MSTN^{-/-}$+AAC groups at 10 weeks after AAC, but there was no significant difference between the rats from the WT and $MSTN^{-/-}$ groups (Table 1). It seemed that AAC resulted in more severe hypertrophic phenotype in $MSTN^{-/-}$ rat than in WT rat. Histological indices revealed that compared with the WT+AAC group, heart size, cardiomyocyte area, and the ratio of heart weight/body weight were significantly raised in the $MSTN^{-/-}$+AAC group (Figures 1A–1D). Furthermore, enlarged cardiomyocyte areas were also detected in angiotensin II (Ang II, a pharmacological agonist, was able to induce cardiac hypertrophy)-treated primary cultured neonatal rat cardiomyocytes. Interestingly, successfully silencing MSTN (Figure S2) *in vitro* could further aggravate the effect of Ang II (Figure 1E). Next, we detected hypertrophic biomarker proteins including brain natriuretic peptide (BNP) and β - myosin heavy chain (β-MHC). The *in vivo* (heart) and *in vitro* (cardiomyocyte) data showed that KO or silenced MSTN dramatically promoted BNP and β-MHC expression (Figures 1F–1I). These data suggested that MSTN deficiency sensitized rat to hypertrophic stimuli and developed a much more severe pathological cardiac hypertrophy.

Both *MSTN*$^{-/-}$ Rat and Silenced MSTN Cardiomyocytes Were More Susceptible to Autophagy

At present, a consensus is emerging in the field that excessive autophagy induced by pressure overload can promote the development of cardiac hypertrophy. We analyzed the ultrastructure of the myocardia by using transmission electron microscopy. Electron microscopic analysis showed that the number of autophagic vacuoles was increased significantly in the $MSTN^{-/-}$+AAC group compared with the WT+AAC group (Figure 2A). To further assess autophagosome formation and the autophagosome-lysosome fusion process, we transfected cardiomyocytes with a construct expressing monomeric red fluorescent protein/green fluorescent protein (mRFP-GFP) tandem-tagged LC3 protein to examine the autophagosome maturation process. In merged images, the yellow and red puncta represented autophagosomes and autolysosomes, respectively, because mRFP, but

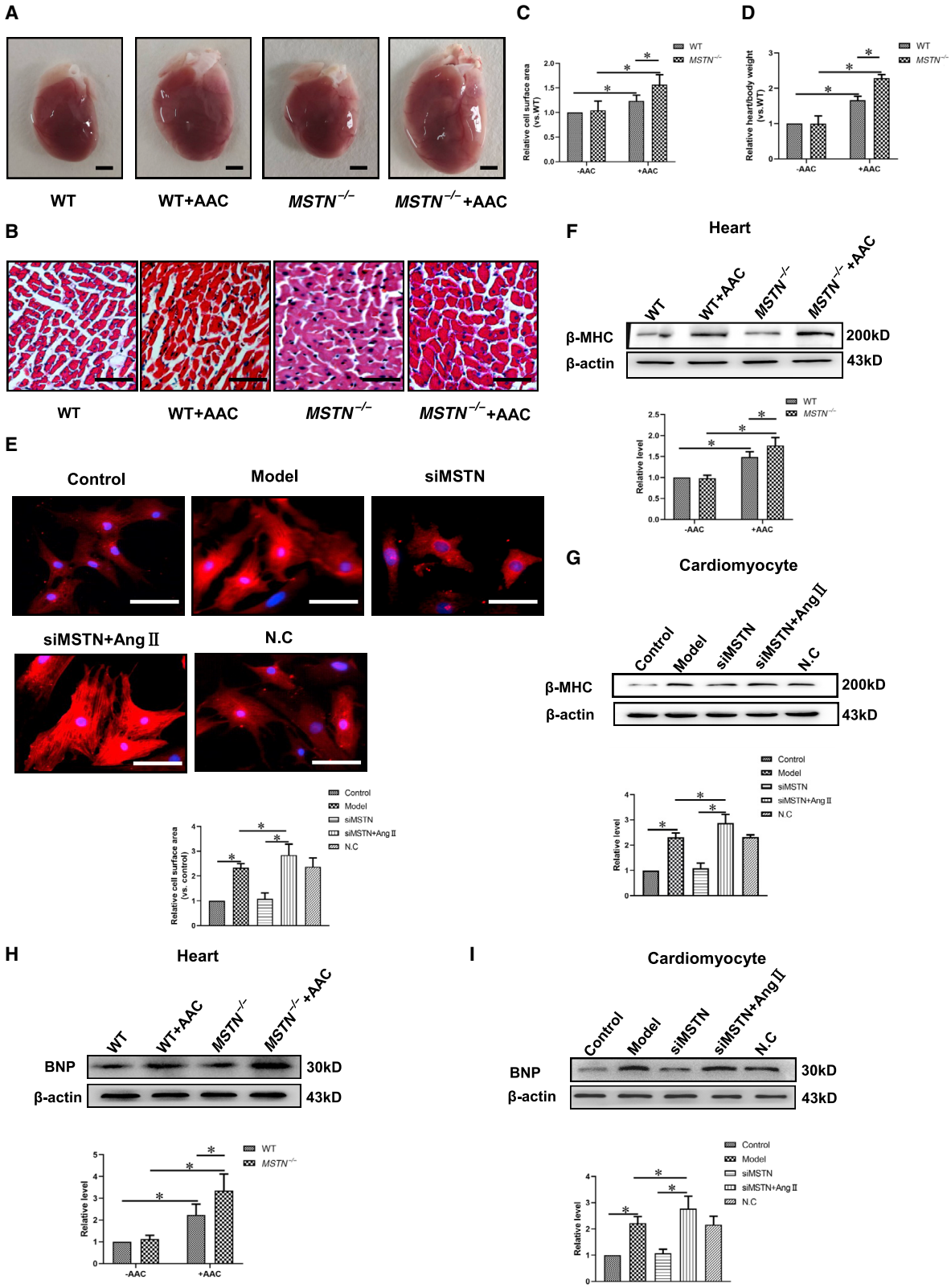

(legend on next page)

not GFP, retained fluorescence in the acidic environment of lysosomes. We observed that the number of autophagosomes was rapidly increased in the silencing MSTN (siMSTN)+Ang II group compared with the model group (Figure 2B). Simultaneously, several recognized autophagic marker proteins, including LC3-II, Beclin-1, and p62, were detected by western blot. Consistent with the results of electron microscopic analysis, there were more increases in LC3-II and Beclin-1 protein expression, as well as more reduction in p62 protein expression in *MSTN*$^{-/-}$+AAC and siMSTN+Ang II groups in both transgenic hearts and cell preparation compared with the WT+AAC and model groups (Figures 2C–2H). These results implied that MSTN deletion was less resistant to autophagy stimulation and produced a much more severe cardiac autophagy *in vivo* and *in vitro*.

MSTN Attenuated Cardiac Hypertrophy and Autophagy

Considering the above results, a question we asked was whether MSTN in cardiac hypertrophy was a suppressor to hypertrophic cardiac injuries or was merely a bystander or a consequence of cardiac hypertrophy. To clarify this issue, we investigated the effects of MSTN on cardiac function and autophagy. To detect the anti-autophagy of MSTN against cardiac hypertrophy condition, we explored the best concentrations of MSTN *in vivo* and *in vitro*. As shown in Figures S3A–S3D, hypertrophic biomarker proteins, including β-MHC and BNP, were decreased by MSTN at the dosage of 50 μg/kg/day and 500 ng/mL *in vivo* and *in vitro*, respectively. At the same time, 50 μg/kg/day MSTN could not cause skeletal muscle damage from rats, and 500 ng/mL MSTN could not damage neonatal rat cardiomyocytes (Figures S3E–S3G). Therefore, the dosage of 50 μg/kg/day and 500 ng/mL MSTN was used in the subsequent experiments *in vivo* and *in vitro*, respectively. Compared with WT rats, AAC induced obvious increases in cardiac hypertrophy, heart weight/body weight, and cardiomyocytes areas (Figures 3A–3D). Meanwhile, cultured neonatal rat cardiomyocytes size was amplified by treatment with Ang II (Figures 3E–3F). However, the AAC and Ang II-induced increases in these indices in WT rats and neonatal rat cardiomyocytes were greatly attenuated by MSTN. Furthermore, AAC- and Ang II-induced increases in hypertrophic marker proteins BNP and β-MHC and autophagic marker proteins LC3-II and Beclin-1, as well as decreases in p62, were also dramatically blunted by MSTN (Figures 3G–3P). Collectively, these results suggested that MSTN could closely impact on the development of cardiac hypertrophy and excessive cardiac autophagy in response to pressure overload.

MSTN Attenuated Cardiac Hypertrophy and Autophagy via the AMPK/mTOR Pathway

As we know, AMPK/mTOR is critical in the regulation of autophagy. To further elucidate the signaling mechanisms by which MSTN acts as a negative regulator in cardiac hypertrophy, we performed western blot on signaling molecules including AMPK, the AMPK phosphorylation target downstream signal mTOR, and cardiac hypertrophic and autophagic marker proteins. First, to establish the cause-consequence relationship between AMPK and mTOR, we modulated AMPK with agonists (A769662) and inhibitors (compound C), and downstream mTOR was evaluated by western blot. Our results demonstrated that A769662 could decrease mTOR expression, and this effect could be reversed by compound C (Figure S4). Second, our results demonstrated that there were more increases in phosphorylated (P)-AMPK protein expression, as well as more reduction in P-mTOR protein expression in *MSTN*$^{-/-}$+AAC and siMSTN+Ang II groups (Figures 4A and 4D). These results indicated that the AMPK/mTOR pathway might accelerate the process of cardiac autophagy in the setting of MSTN deletion. Third, to further confirm the regulation of MSTN to cardiac hypertrophy and autophagy via the AMPK/mTOR pathway, we silenced mTOR to test whether MSTN regulated cardiac autophagy in mediating the inhibitory effect on cardiac hypertrophy. We found that small interfering RNA (siRNA) targeting mTOR suppressed the protecting effect of MSTN on cardiac hypertrophy (Figures 4E and 4F). Simultaneously, silencing mTOR (Figure S5) also dramatically abolished the inhibitory effect of MSTN on cardiac autophagy (Figures 4G–4I). Finally, the *in vivo* and *in vitro* results demonstrated that MSTN significantly repressed P-AMPK protein expression and promoted expression of P-mTOR and its downstream protein p70S6k (Figures 4J–4O). Taken together, our data suggested that MSTN blocked excessive cardiac autophagy partially through the AMPK/mTOR pathway, thereby repressing cardiac hypertrophy development.

MSTN Attenuated Cardiac Hypertrophy and Autophagy via the PPARγ/NF-κB Pathway

As already mentioned, in addition to the AMPK/mTOR pathway, other pathways such as the PPARγ/NF-κB pathway are also crucially involved in the regulation of cardiac autophagy and hypertrophy.[24] To understand another signal pathway associated with the cardiac autophagy and hypertrophy regulated by MSTN, we examined the expression of PPARγ, NF-κB, and cardiac hypertrophic and

Figure 1. Abdominal Aorta Coarctation (AAC) and Ang II-Induced Cardiac Hypertrophy Were Aggravated in MSTN Knockout Rats and Silenced MSTN Cardiomyocytes

(A) Representative heart gross morphology from WT, WT+AAC, *MSTN*$^{-/-}$, and MSTN$^{-/-}$+AAC rats subjected to AAC or sham operation (scale bars represent 2 mm). (B) Histological sections were stained with hematoxylin and eosin (H&E) to analyze the cell surface area (scale bars represent 50 μm). (C) Quantitative data of relative cell surface area (n = 100 cardiomyocytes per animal, 6 rats/group) and normalized by the cell number. (D) Quantitative data of relative heart-to-body weight (n = 6 rats/group). (E) Representative microphotographs of cardiomyocytes surface area. Cardiomyocyte was identified with sarcomeric α-actin antibody (red signal), and the nucleus was identified by DAPI (blue signal) (scale bars represent 50 μm). Cell size in cardiomyocytes transduced was analyzed with Image-Pro Plus 6.0 and normalized by the cell number (n = 600 cardiomyocytes per group). (F) Western blot assay for β-MHC expression in rat hearts in the indicated groups. (G) Western blot assay for β-MHC expression in cultured neonatal rat cardiomyocytes in the indicated groups. (H) Western blot assay for BNP expression in rat hearts in the indicated groups. (I) Western blot assay for BNP expression in cultured neonatal rat cardiomyocytes in the indicated groups. The average data were represented by mean ± SD (n = 6 rats/group or independent experiments in each cell culture experiment). *$p < 0.05$.

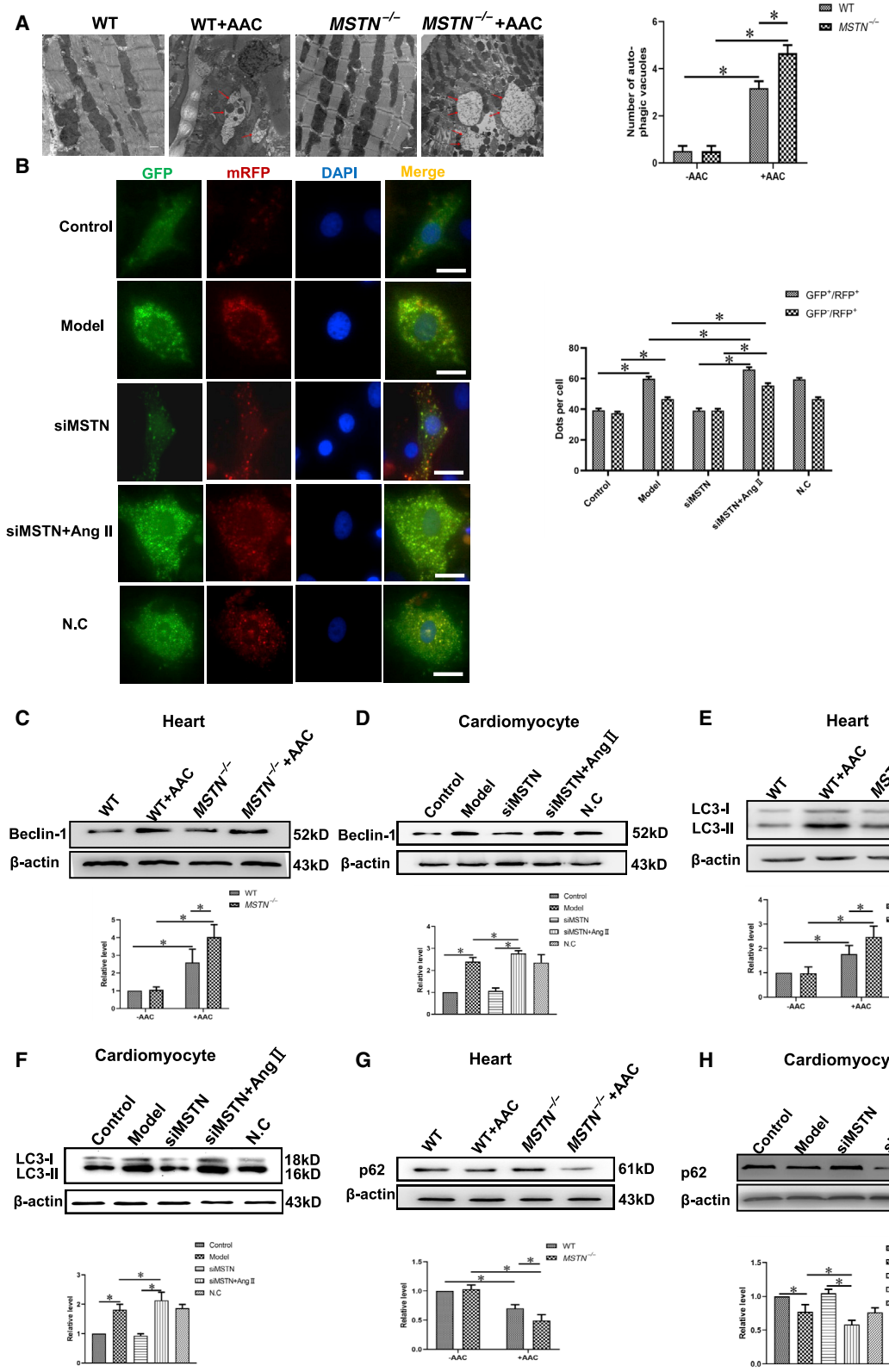

(legend on next page)

autophagic marker proteins. Consistent with the AMPK/mTOR pathway, KO (*in vivo*) or silenced MSTN (*in vitro*) caused more increases in NF-κB protein expression, as well as more reduction in PPARγ protein expression, in $MSTN^{-/-}$+AAC and siMSTN+Ang II groups (Figures 5A–5D). Simultaneously, MSTN could promote PPARγ protein expression (Figure S6). These results revealed that the PPARγ/NF-κB pathway also participated in the modification of cardiac autophagy and hypertrophy. Especially under the MSTN deficiency circumstance, the PPARγ/NF-κB pathway might speed up the process of cardiac autophagy and the development of cardiac hypertrophy. To further test the hypothesis that MSTN played an essential role in mediating cardiac autophagy and hypertrophy by the PPARγ/NF-κB pathway, we silenced PPARγ (Figure S7) to monitor hypertrophy- and autophagy-related marker protein expression. As Figures 5E and 5F show, MSTN could significantly inhibit hypertrophy marker proteins (β-MHC and BNP) expression *in vivo* and *in vitro*. At the same time, MSTN suppressed autophagy-related marker proteins (LC3-II and Beclin-1) and NF-κB protein expression, but likewise promoted p62 (another autophagy-related marker protein) expression (Figures 5G–5J). However, silencing PPARγ could reverse the above results induced by MSTN. In summary, our data suggested that MSTN blocked excessive cardiac autophagy at least partly through the PPARγ/NF-κB pathway, thereby restraining cardiac hypertrophy development.

miR-128 Pro-hypertrophic and Pro-autophagic Effects through Directly Targeting PPARγ

Zeng et al.[25] reported that miR-128 inhibition attenuated myocardial ischemia/reperfusion injury-induced cardiomyocyte apoptosis, indicating the detrimental effect of miR-128 on myocardial cells. In our study, the effect of miR-128 on neonatal rat cardiomyocyte hypertrophy was evaluated by β-MHC and BNP protein expression. Treatment of neonatal rat cardiomyocyte with 100 nmol/L Ang II led to significant increases in β-MHC and BNP protein expression, which was elevated by overexpression of miR-128, whereas co-transfection with antisense inhibitor oligonucleotide AMO-128 (the specific inhibitor of the miR-128) abrogated the effect of miR-128 (Figures 6A and 6B). Similarly, Ang II (100 nmol/L) also upregulated autophagy-related marker protein levels of LC3-II and Beclin-1, and downregulated p62 protein expression. Transfection with miR-128 promoted Ang II-induced LC3-II and Beclin-1 upregulation and p62 downregulation, which were abolished by co-transfection of AMO-128 (Figures 6C–6E). Interestingly, when treated only with miR-128, there are no effects on cardiac hypertrophy (Figures S8A and S8B) and autophagy (Figures S8C–S8E). At the same time, we evaluated the effect of miR-128 on MSTN. Our results indicated that miR-128 could not inhibit MSTN expression in cardiomyocytes (Figure S8F).

In the subsequent experiments, we further used TargetScan software to predict a conserved binding site for miR-128 in the 3′ UTR of the PPARγ gene (Figure S9). miR-128 was transfected into cultured neonatal rat cardiomyocyte to test this binding profile, and the results showed that the decreasing protein levels of PPARγ induced by Ang II were more reduced. Conversely, PPARγ protein was significantly upregulated when AMO-128 was transfected into neonatal rat cardiomyocyte, indicating that PPARγ was negatively regulated by miR-128 (Figure 6F). To further verify that miR-128 directly targeted PPARγ, we prepared luciferase constructs carrying the PPARγ 3′ UTR (Figure 6G). Co-transfection of miR-128 with the luciferase reporter vector into HEK293 cells caused a sharp decrease in luciferase activity compared with transfection of the luciferase vector alone. The miR-128-induced depression of luciferase activity was rescued by mut-PPARγ. These results experimentally revealed that PPARγ was a direct target of miR-128.

Effects of MSTN on the Expression of miR-128

Here, to detect the relationship between MSTN and the miR-128 signal pathway, we assessed the expression of miR-128 by quantitative real-time PCR. Our results revealed that miR-128 was significantly more increased in KO MSTN rat heart and silenced MSTN neonatal rat cardiomyocyte (Figures 7A and 7B), whereas MSTN significantly decreased miR-128 expressions in both transgenic hearts and cell preparation (Figures 7C and 7D).

DISCUSSION

Cardiac hypertrophy is a common pathological feature of some major cardiovascular diseases, such as hypertension and myocardial infarction, and is strongly associated with a significant increase in the risk for heart failure and sudden cardiac death. However, very little is known about the role of MSTN in cardiac hypertrophy induced by abdominal aortic constriction. In the present study, we provide a novel understanding of MSTN on molecular events of cardiac hypertrophy and ventricular dysfunction after abdominal aortic constriction.

There are two major findings of the current study. First, MSTN deficiency in rats exacerbated AAC-induced cardiac hypertrophy and

Figure 2. AAC and Ang II-Induced Cardiac Autophagy Were Aggravated in MSTN Knockout Rats and Silenced MSTN Cardiomyocytes

(A) Ultrastructural examination of cardiomyocytes after AAC from WT and $MSTN^{-/-}$ rat hearts by electronic microscopy (scale bars represent 500 nm). Arrows indicate autophagy vacuoles. (B) Cultured neonatal rat cardiomyocytes transiently expressing mRFP-GFP-LC3 were transfected with NC or siMSTN mimics as indicated. The cells were visualized by confocal microscopy (scale bars represent 20 μm). The number of GFP^+/RFP^+ (yellow) and GFP^-/RFP^+ (red) dots per cell was quantified using Image-Pro Plus 6.0. (C) Western blot assay for Beclin-1 expression in rat hearts in the indicated groups. (D) Western blot assay for Beclin-1 expression in cultured neonatal rat cardiomyocytes in the indicated groups. (E) Western blot analysis of the levels of LC3 in rat hearts in the indicated groups. (F) Western blot analysis of the levels of LC3 in cultured neonatal rat cardiomyocytes in the indicated groups. (G) Western blot assay for p62 expression in rat hearts in the indicated groups. (H) Western blot assay for p62 expression in cultured neonatal rat cardiomyocytes in the indicated groups. The average data were represented by mean ± SD (n = 6 rats/group or independent experiments in each cell culture experiment). *$p < 0.05$.

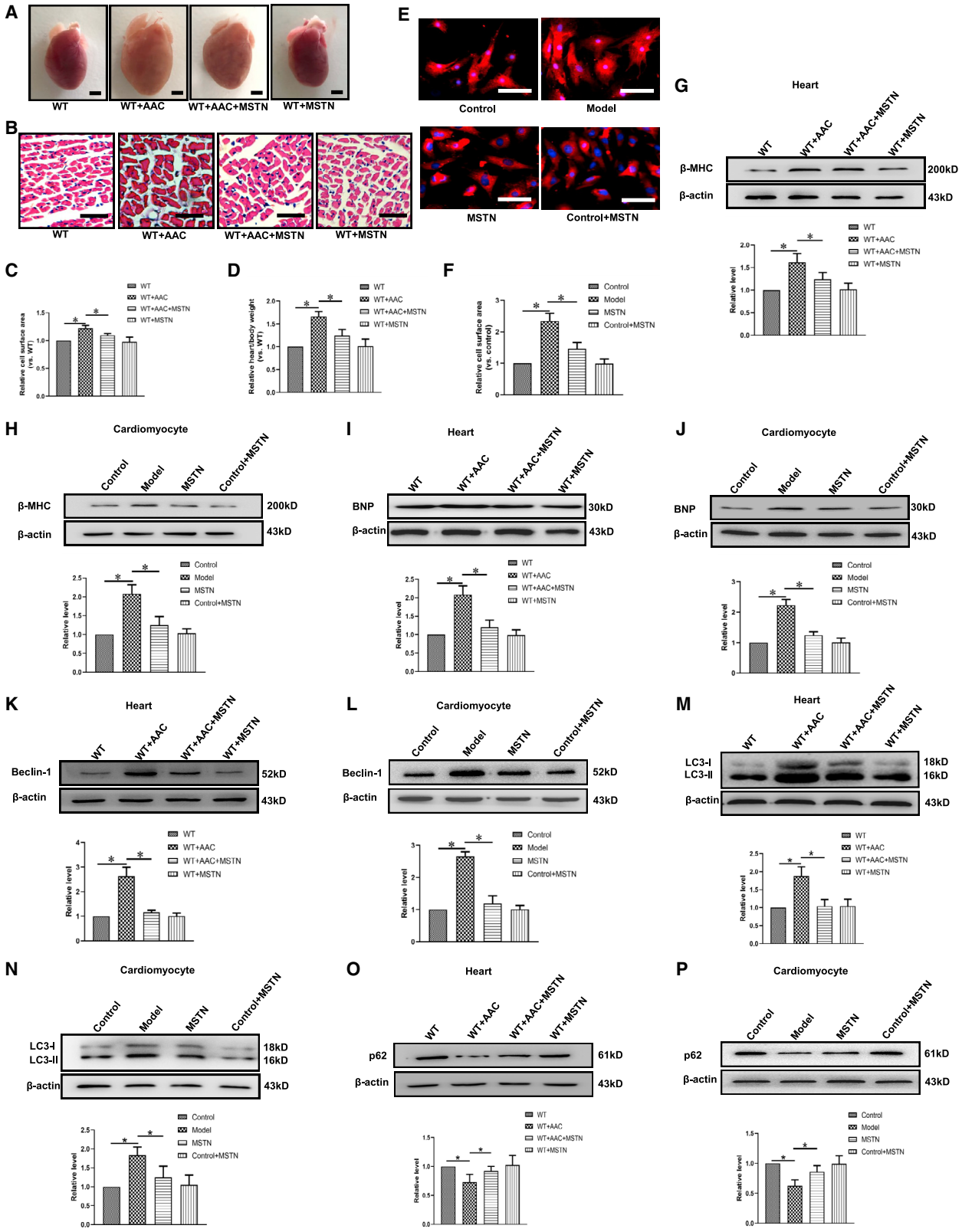

(legend on next page)

dysfunction. Antithetically, AAC-produced hypertrophic phenotypes were significantly attenuated by MSTN activation. Second, MSTN exerted an inhibitory effect on stress-induced cardiac hypertrophy, most likely suppressing excessive cardiomyocytes autophagy through AMPK/mTOR and miR-128/PPARγ/NF-κB pathways.

Autophagy is evolutionarily utilized by eukaryotic cells to recycle cellular waste into reusable, biologically active monomers and thereby maintain homeostasis.[26,27] Essentially, it is a normal physiological process, but the uncontrolled autophagic response plays a crucial role in pathophysiological changes of various diseases.[28–30] Some recent studies have suggested that high levels of autophagy may aggravate cardiac hypertrophy. Our data showed that rat induced by AAC for 10 weeks or neonatal rat cardiomyocytes stimulated with Ang II over 24 h resulted in hypertrophic phenotypes, in parallel with excessive cardiomyocytes autophagy, suggesting potential involvement of cardiac autophagy in the development of cardiac hypertrophy. Interestingly and surprisingly, in AAC or Ang II-induced cardiac hypertrophy, cardiac autophagy (*in vivo* and *in vitro*) was aggravated in $MSTN^{-/-}$ rats and silencing MSTN cardiomyocytes, whereas AAC or Ang II-induced cardiac or cardiomyocytes injury and excessive cardiomyocytes autophagy were greatly attenuated in rats or cardiomyocytes treatment with MSTN, respectively. However, MSTN KO did not produce spontaneous cardiac hypertrophy, which could have contributed to a compensative effect of other molecular regulators, in the complex organisms of the heart, on the loss of MSTN function in $MSTN^{-/-}$ rat. Nevertheless, we demonstrated that MSTN acted as an endogenous cardioprotective regulator against pressure. These results strongly indicated that MSTN exerted a protective effect against stress-induced cardiac hypertrophy via inhibition of excessive cardiomyocytes autophagy.

Autophagy in cardiomyocytes is a complex process that can be controlled by several signaling pathways. The AMPK/mTOR is one of the major pathways to regulate autophagy. Meanwhile, Zhang et al.[31] reported that MSTN negatively regulated the levels of AMPK in peripheral tissues, and thus influenced insulin sensitivity. To further delineate the potential mechanisms by which MSTN exerted a protective effect on stress-induced cardiac hypertrophy, we first investigated the AMPK/mTOR signaling pathway leading to autophagy activation. The data obtained from both *in vivo* and *in vitro* experiments pointed out that the stress-induced increase in phosphorylated levels of AMPK and decrease in phosphorylated levels of mTOR were further aggravated by MSTN KO in rat or in MSTN knocking down neonatal rat cardiomyocytes; conversely, upregulated activity of AMPK signaling by AAC or Ang II was greatly attenuated by treatment with MSTN. This result strongly revealed that there was an inevitable signal conditioning relationship between MSTN and the AMPK/mTOR pathway. More importantly, stress-induced cardiac hypertrophy and excessive autophagy could be ameliorated by treatment with MSTN both *in vivo* and *in vitro*, and this effect was abolished in mTOR knocking down neonatal rat cardiomyocytes. These results together suggested that MSTN could inhibit excessive cardiac autophagy by blockade of the AMPK/mTOR pathway.

NF-κB is known to control multiple cellular processes, and several molecules involved in autophagy are dependent on NF-κB.[32,33] Moreover, cumulative evidence indicated that PPARγ could suppress NF-κB activation by several mechanisms and then repress NF-κB-mediated transcription for certain inducible genes.[34] Therefore, we tested whether the effects of MSTN, inhibition of cardiac hypertrophy and excessive autophagy, were also linked to the PPARγ/NF-κB pathway. First, we found that in $MSTN^{-/-}$ rat under AAC or in MSTN knocking down neonatal rat cardiomyocytes treatment with Ang II, the PPARγ expression was more decreased and NF-κB more increased, whereas this effect could be reversed in PPARγ knocking down neonatal rat cardiomyocytes. Indeed, this result strongly implied that the PPARγ/NF-κB signaling pathway was also involved in the regulation of cardiac hypertrophy and autophagy by MSTN. Further, when the PPARγ was silenced by siRNA technique, the effect of MSTN on anti-hypertrophic and anti-autophagy was abrogated. Similarly, these results together revealed that PPARγ/NF-κB was another anti-hypertrophic and anti-autophagy signaling pathway regulated by MSTN.

miRNAs, as regulators of a wide range of biological processes, often participated in the pathogenesis of specific diseases, including heart disease.[35,36] However, no direct evidence indicates the role of MSTN and miR-128 or the underlying regulatory mechanisms between MSTN and miR-128 in the pathological process of cardiac hypertrophy. In this study, MSTN remarkably decreased the expression of miR-128 compared with the model of cardiac hypertrophy. Indeed, this result strongly revealed that there was an inevitable

Figure 3. MSTN Attenuated Cardiac Hypertrophy and Autophagy

(A) Representative heart gross morphology from WT, WT+AAC, WT+AAC+MSTN, and WT+MSTN rats subjected to AAC or sham operation (scale bars represent 2 mm). (B) Histological sections were stained with H&E to analyze the cell surface area (original magnification ×200, scale bars represent 50 μm). (C) Quantitative data of relative cell surface area (n = 100 cardiomyocytes per animal, 6 rats/group). (D) Quantitative data of relative heart-to-body weight. (E) Representative microphotographs of cardiomyocytes surface area. Cardiomyocyte was identified with sarcomeric α-actin antibody (red signal), and the nucleus was identified by DAPI (blue signal) (scale bars represent 50 μm). (F) Summarized data of cell surface area (n = 600 cardiomyocytes per group). (G and H) Western blot assay for β-MHC expression in rat hearts (G) and cultured neonatal rat cardiomyocytes (H) in the indicated groups. (I and J) Western blot assay for BNP expression in rat hearts (I) and cultured neonatal rat cardiomyocytes (J) in the indicated groups. (K and L) Western blot assay for Beclin-1 expression in rat hearts (K) and cultured neonatal rat cardiomyocytes (L) in the indicated groups. (M and N) Western blot analysis of the levels of LC3 in rat hearts (M) and cultured neonatal rat cardiomyocytes (N) in the indicated groups. (O and P) Western blot assay for p62 expression in rat hearts (O) and cultured neonatal rat cardiomyocytes (P) in the indicated groups. The average data were represented by mean ± SD (n = 6 rats/group or independent experiments in each cell culture experiment). *$p < 0.05$.

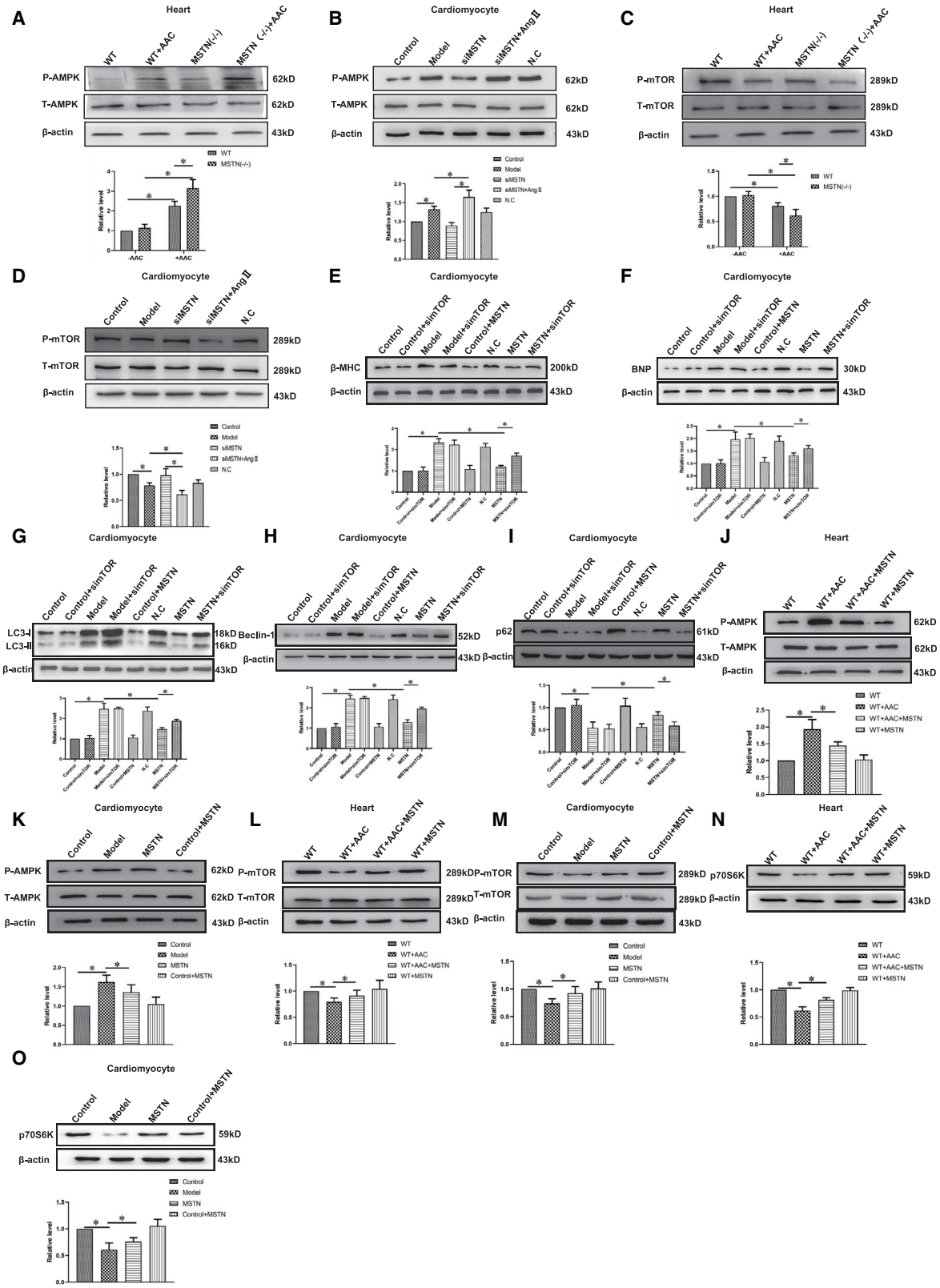

(legend on next page)

signal conditioning relationship between MSTN and miR-128. In addition, we used both gain- and loss-of-function techniques on miR-128 expression to explore the regulatory effect of miR-128 on pro-hypertrophy action. We found that forcing overexpression of miR-128 could significantly promote the development of cardiac hypertrophy and excessive cardiac autophagy *in vitro*. On the contrary, these changes could be significantly reversed by AMO-128. Furthermore, to explore direct miR-128 targeting, we used miRanda software to predict the target genes of miR-128. We also found that PPARγ was most likely a target gene for the miR-128 simply because of the conservative sequence fragment among different species, which was fully supported by the notion that, by using a luciferase reporter gene assay, as well as protein expression detections, PPARγ as a direct target of miR-128 was validated. Taking all of the data together reported here suggested that miR-128 promoted cardiac hypertrophy via targeting PPARγ and could be repressed by MSTN.

In summary, we demonstrate that MSTN significantly blunts pathological cardiac hypertrophy and dysfunction, at least in part, by inhibiting excessive cardiac autophagy via the AMPK/mTOR and miR-128/PPARγ/NF-κB signaling pathways, as summarized in Figure 8. These findings suggest that MSTN may be a potential therapeutic target for the prevention and treatment of cardiac hypertrophy and heart failure.

MATERIALS AND METHODS

Creation of MSTN KO Rat and Sequencing Confirmation

MSTN KO rats were constructed, and detailed information was as described in Yong's paper.[37] In brief, Zinc Finger Nuclease (ZFN) constructs were designed to target the genomic region around rat mstn exon 1 and were tested for their efficiency in the rat cell line. Then ZFN construct was injected in one-cell fertilized eggs. Injected eggs were transferred to pseudopregnant females. Next, to identify the modifications in founders, we extracted genomic DNA from the tails of newborn (10 d) rats using the salting-out method. PCR was performed to amplify the MSTN sequence with the primers 5′-GGCA TGGTAATGATTGTTTCCGTG-3′ (forward) and 5′-TTTACCTGT TTGTGCTGATTGCTGC-3′ (reverse). Then the PCR products were digested by ClaI restriction endonuclease at 30°C overnight and fractioned on a 2% agarose gel.

Pressure Overload-Induced Cardiac Hypertrophy

All experimental procedures conformed to the *Guide for the Care and Use of Laboratory Animals* (Eighth Edition, 2011) published by the NIH. This study, including any relevant details, was approved by the Experimental Animal Ethic Committee of Harbin Medical University. AAC was performed by following previously described methods.[38] In brief, age- and sex-matched rats were anesthetized with sodium pentobarbital (40 mg/kg intraperitoneally [i.p.]), and the abdomen was opened on aseptic conditions. Under sterile conditions, the abdominal aorta was separated for a 1-cm segment above the double renal artery. Then AAC was achieved by tying a 7-0 silk suture around the abdominal aorta against a diameter of 0.5-mm silver needle. After ligation, the needle was gently removed before the abdomen was sutured. The rats were divided into six groups randomly: WT group (underwent laparotomy only, not for abdominal aortic constriction); WT+AAC group (underwent laparotomy; abdominal aortic constriction for 10 weeks); $MSTN^{-/-}$ group (underwent laparotomy only, not for abdominal aortic constriction); $MSTN^{-/-}$+AAC group (underwent laparotomy; abdominal aortic constriction for 10 weeks); WT+AAC+MSTN group (underwent laparotomy and abdominal aortic constriction, then injected i.p. with MSTN [120-00; PeproTech] at 50 μg/kg/day for 10 weeks by subcutaneous injection); and WT+MSTN group (injected i.p. with MSTN at 50 μg/kg/day for 10 weeks).

Echocardiography

Echocardiography was performed using a VisualSonics Vevo 2100 instrument (VisualSonics, Canada) at the indicated time to evaluate the cardiac function of the rats, as previously reported.[39] After anesthetization with sodium pentobarbital (40 mg/kg i.p.), the rats were placed in a supine position. A 6-MHz transducer was applied to the left hemithorax. The hearts were imaged in the short-axis view at the papillary muscle level of the left ventricle. LVPWd, LVPWs, IVSd, IVSs, LVFS, and LVEF were calculated.

Electron Microscopy

The small pieces of fresh heart tissue were immersed in universal fixative (1% glutaryl-aldehyde, 4% paraformaldehyde [pH 7.4]) immediately after biopsy, postfixed in 2% osmium tetroxide, dehydrated in graded acetone, and embedded in an Epon-Araldite mixture. Selected blocks were thin sectioned, mounted on copper grids, and contrasted with uranyl acetate and lead citrate. The grids were examined in a Hitachi H7650 transmission electron microscope (Hitachi, Tokyo, Japan). Quantitative analysis of autophagosomes was carried out using 10 images from different fields, with the investigator blinded as to the origin of each image. Autophagosomes or autolysosomes were identified by the characteristic

Figure 4. MSTN Attenuated Cardiac Hypertrophy and Autophagy via the AMPK/mTOR Pathway

(A and B) Western blot assay for P-AMPK expression in rat hearts (A) and cultured neonatal rat cardiomyocytes (B) in the indicated groups. (C and D) Western blot assay for P-mTOR expression in rat hearts (C) and cultured neonatal rat cardiomyocytes (D) in the indicated groups. (E and F) Western blot assay for β-MHC (E) and BNP (F) expression in cultured neonatal rat cardiomyocytes in the indicated groups. (G–I) Western blot analysis of the levels of LC3 (G), Beclin-1 (H), and p62 (I) in cultured neonatal rat cardiomyocytes in the indicated groups. (J and K) Western blot assay for P-AMPK expression in rat hearts (J) and cultured neonatal rat cardiomyocytes (K) in the indicated groups. (L and M) Western blot assay for P-mTOR expression in rat hearts (L) and cultured neonatal rat cardiomyocytes (M) in the indicated groups. (N and O) Western blot assay for p70S6K expression in rat hearts (N) and cultured neonatal rat cardiomyocytes (O) in the indicated groups. The average data were represented by mean ± SD (n = 6 rats/group or independent experiments in each cell culture experiment). *$p < 0.05$.

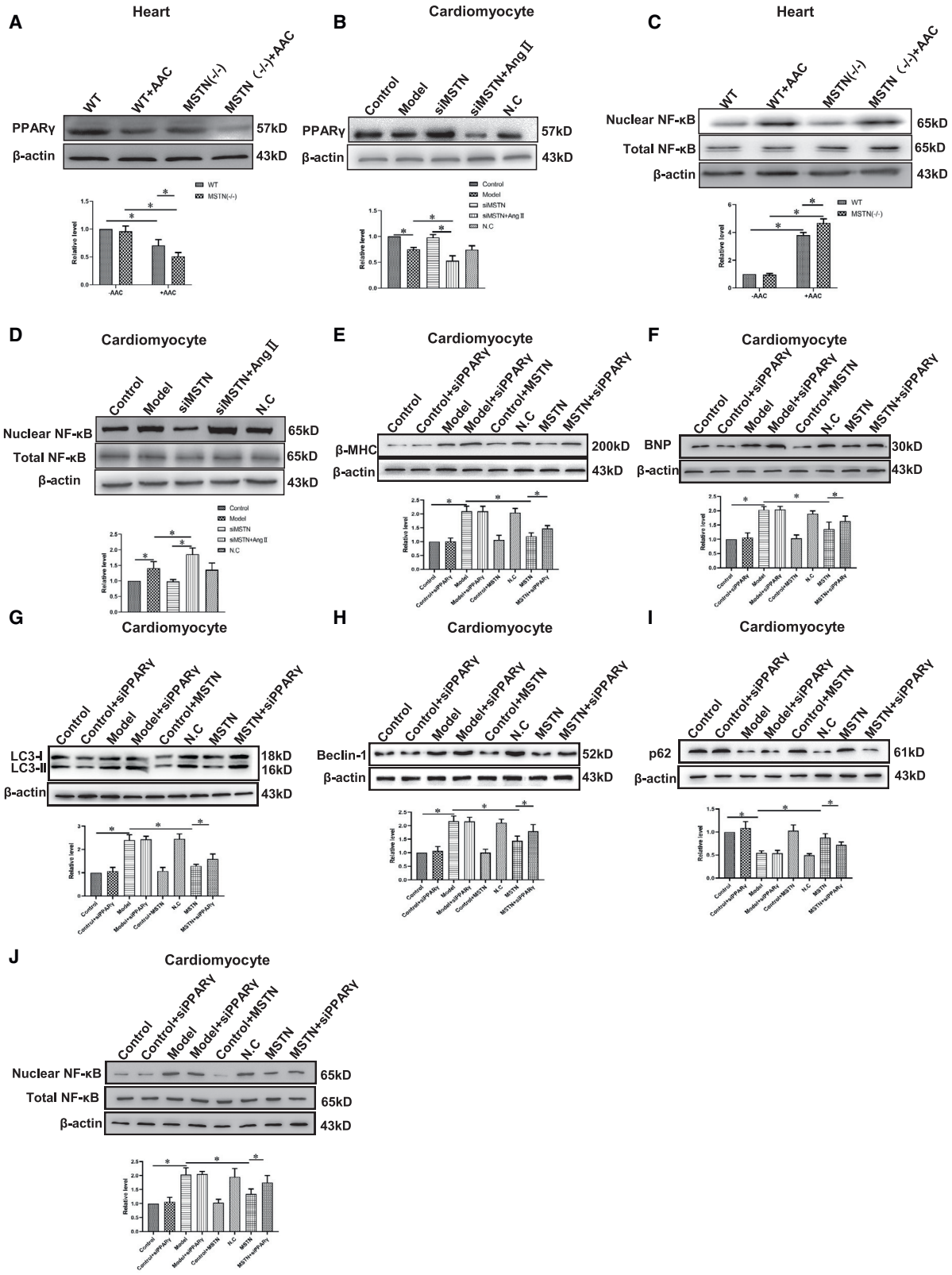

(legend on next page)

structure of a double- or multi-lamellar smooth membrane completely surrounding compressed mitochondria or membrane-bound electron-dense material.

Hematoxylin and Eosin Staining

The hearts were excised from animals sacrificed 10 weeks after the AAC or sham operation; then paraffin-embedded hearts were sectioned. These sections were stained with hematoxylin and eosin (H&E), and the histopathological abnormalities were investigated under the light microscope. The photographs were captured with an Olympus BX60 microscope (Olympus Optical, Tokyo, Japan). Ten myocytes were randomly selected per field of view from about 10 fields of view of each heart sample at a magnification ×200. Finally, quantitative analyses were performed by using a quantitative digital image analysis system (Image-Pro Plus 6.0).

Neonatal Rat Cardiomyocytes Culture and Adenoviral Infection

Neonatal rat cardiomyocytes were isolated and cultured as described.[40] In brief, neonatal rat cardiomyocytes were prepared from 2- to 3-day-old neonatal Wistar rats. The neonatal rats were anesthetized with dry ice (CO_2) and then immersed in 75% (v/v) ethanol. The ventricles were finely minced and placed together in 0.25% trypsin. Collected cell suspensions were centrifuged and resuspended in DMEM (GIBCO and Thermo Fisher Scientific) supplemented with 10% fetal bovine serum (FBS; GIBCO and Thermo Fisher Scientific). Then all cells were cultured at 37°C with 5% CO_2 followed by a 90-min preplating (in order to eliminate the few non-myocyte cells remaining). After 90-min preplating, the cell suspensions were transferred to the other culture flask. To inhibit non-cardiomyocyte cell proliferation, we added bromodeoxyuridine (BrdU) (0.1 mmol/L) throughout the culture period. Cardiomyocyte cultures thus obtained were more than 95% pure, as revealed by observation of their contractile characteristics under a phase-contrast microscope. Neonatal rat cardiomyocytes were randomly divided into 18 groups: (1) control group; (2) model group, neonatal rat cardiomyocytes were incubated with Ang II (100 nmol/L) for 24 h; (3) MSTN group, neonatal rat cardiomyocytes were given 500 ng/mL MSTN for 24 h after treatment with Ang II (100 nmol/L) for 24 h; (4) siMSTN group, neonatal rat cardiomyocytes were transfected with siMSTN (10 nmol/L) for 24 h; (5) siMSTN+Ang II group, neonatal rat cardiomyocytes were transfected with siMSTN (10 nmol/L) for 24 h before exposure to Ang II (100 nmol/L); (6) MSTN+simTOR, neonatal rat cardiomyocytes were transfected with simTOR (10 nmol/L) for 24 h before exposure to 500 ng/mL MSTN for 24 h, following 24-h treatment with Ang II (100 nmol/L); (7) MSTN+siPPARγ group, neonatal rat cardiomyocytes were transfected with siPPARγ (10 nmol/L) for 24 h before exposure to 500 ng/mL MSTN for 24 h, following 24-h treatment with Ang II (100 nmol/L); (8) miR-128 group, neonatal rat cardiomyocytes were transfected with miR-128 (50 nmol/L) for 24 h after treatment with Ang II (100 nmol/L) for 24 h; (9) AMO-128 group, neonatal rat cardiomyocytes were co-transfected with miR-128 (50 nmol/L) and AMO-128 (100 nmol/L) for 24 h after treatment with Ang II (100 nmol/L) for 24 h; (10) negative control (NC) group, cells were transfected with a random sequence for 24 h after treatment with Ang II (100 nmol/L) for 24 h; (11) AMO-NC group, cells were transfected with a random sequence for 24 h after treatment with Ang II (100 nmol/L) for 24 h; (12) Control+simTOR group, neonatal rat cardiomyocytes were transfected with simTOR (10 nmol/L) for 24 h; (13) Model+simTOR group, neonatal rat cardiomyocytes were transfected with simTOR (10 nmol/L) for 24 h, following 24-h treatment with Ang II (100 nmol/L); (14) Control+MSTN group, neonatal rat cardiomyocytes were exposed to 500 ng/mL MSTN for 24 h; (15) Control+siPPARγ group, neonatal rat cardiomyocytes were transfected with siPPARγ (10 nmol/L) for 24 h; (16) Model+siPPARγ group, neonatal rat cardiomyocytes were transfected with siPPARγ (10 nmol/L) for 24 h, following 24-h treatment with Ang II (100 nmol/L); (17) Control+miR-128 group, neonatal rat cardiomyocytes were transfected with miR-128 (50 nmol/L) for 24 h; and (18) Control+NC group, neonatal rat cardiomyocytes were transfected with a random sequence for 24 h.

Immunofluorescence Staining

Immunofluorescence staining was performed to detect the neonatal rat cardiomyocytes size. In short, the cells were cultured on coverslips and received the desired treatment. At the end of the treatment, the cells were washed with PBS, fixed with 4% paraformaldehyde, and permeabilized using 0.2% Triton X-100. Cells were incubated with sarcomeric α-actin at 4°C overnight. Then the second antibody was incubated in the dark. In the end, DAPI (Beyotime Biotechnology, Shanghai, China) was counterstained for the identification of nucleus. Photographs were acquired by using fluorescence microscope (Leica, Heidelberg, Germany). Finally, quantitative analyses were performed by using a quantitative digital image analysis system (Image-Pro Plus 6.0).

Luciferase Assays

The PPARγ 3′ UTR containing the miR-128 target sequences (position 82–88) and mutant sequences (a single-base mutant in the 3′ UTR) was chemically synthesized (GenScript, Nanjing, China) and cloned into (HindIII and SacI sites) the pMIR-REPORTTM luciferase miRNA expression reporter vector (Ambion) to form a chimeric plasmid. HEK293 cells were transfected with either PPARγ

Figure 5. MSTN Attenuated Cardiac Hypertrophy and Autophagy via the PPARγ/NF-κB Pathway

(A and B) Western blot assay for PPARγ expression in rat hearts (A) and cultured neonatal rat cardiomyocytes (B) in the indicated groups. (C and D) Western blot assay for NF-κB expression in rat hearts (C) and cultured neonatal rat cardiomyocytes (D) in the indicated groups. (E and F) Western blot assay for β-MHC (E) and BNP (F) expression in cultured neonatal rat cardiomyocytes in the indicated groups. (G–I) Western blot analysis of the levels of LC3 (G), Beclin-1 (H), and p62 (I) in cultured neonatal rat cardiomyocytes in the indicated groups. Western blot assay for NF-κB expression in cultured neonatal rat cardiomyocytes (J) in the indicated groups. The average data were represented by mean ± SD (n = 6 rats/group or independent experiments in each cell culture experiment). *$p < 0.05$.

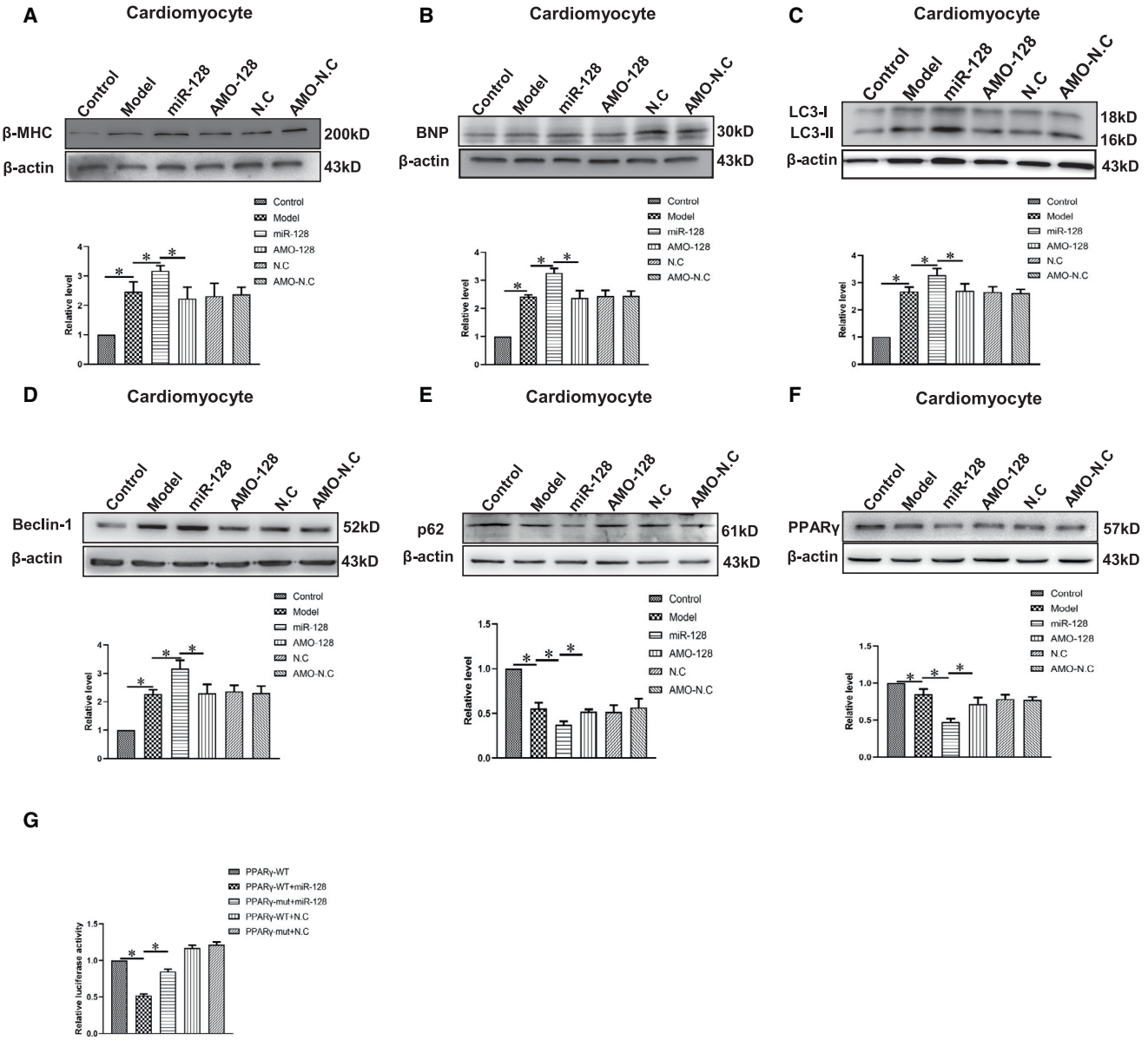

Figure 6. Pro-hypertrophic and Pro-autophagic Effects of miR-128 and Experimental Identification of PPARγ as a Target of miR-128

(A and B) Western blot assay for β-MHC (A) and BNP (B) expression in cultured neonatal rat cardiomyocytes in the indicated groups. (C–E) Western blot analysis of the levels of LC3 (C), Beclin-1 (D), and p62 (E) in cultured neonatal rat cardiomyocytes in the indicated groups. (F) Effect of miR-128 on the protein expression of PPARγ in cultured neonatal rat cardiomyocytes. (G) Luciferase reporter activities of chimerical vectors carrying luciferase gene and a fragment of PPARγ 3′ UTR from rat containing the binding sites of miR-128. The average data were represented by mean ± SD (n = 6 independent experiments in each group). *$p < 0.05$.

3′ UTR-luci-WT or PPARγ 3′ UTR-luci-MUT in 24-well plates using Lipofectamine 2000 transfection reagent according to the manufacturer's instructions, and co-transfected with miR-128 mimic, antagomir-128, or the same concentration of NC. Each well was also co-transfected with the pRL-TK plasmid (Promega) to determine the transfection efficiency. Subsequently, firefly and Renilla luciferase activity levels were measured in cells that were harvested 24 h post-transfection using the Dual-Luciferase Reporter Assay System (Promega Corporation).

Western Blot

Protein samples (50 mg) were separated in SDS-PAGE and transferred onto a nitrocellulose membrane. The blots were blocked with 5% nonfat milk for 2 h at room temperature, then incubated

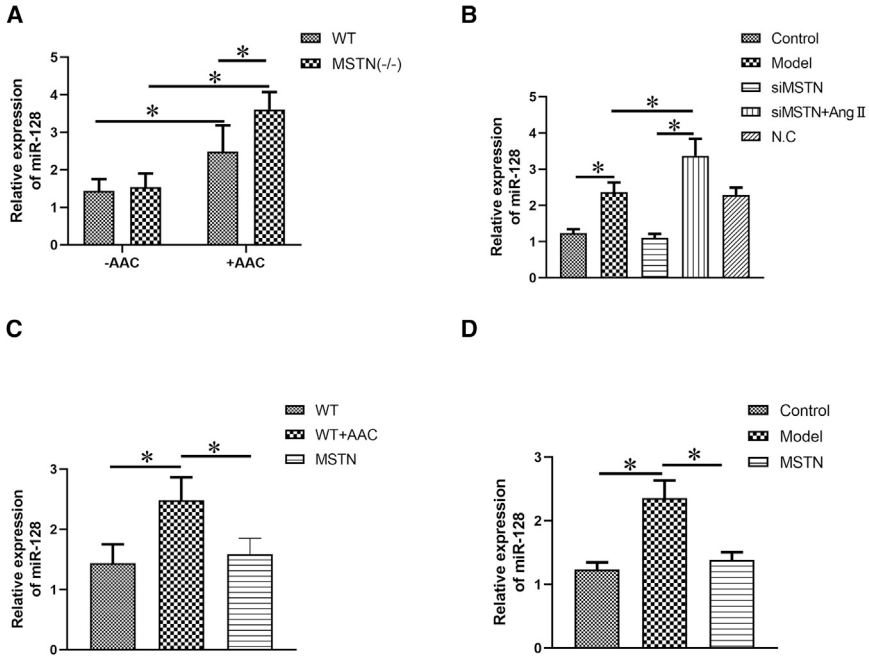

Figure 7. MSTN Inhibited miR-128 Expression *In Vivo and In Vitro*

miR-128 expression was measured by quantitative real-time PCR in rat hearts (A) and cultured neonatal rat cardiomyocytes (B) in the indicated groups. MSTN inhibited miR-128 expression in rat hearts (C) and cultured neonatal rat cardiomyocytes (D) in the indicated groups. The average data were represented by mean ± SD (n = 6 independent experiments in each group), $^{*}P < 0.05$.

with primary antibody including BNP (1:1,000 dilution, sc-271185; Santa Cruz), β-MHC (1:2,000 dilution, SAB2106550; Sigma), Beclin-1 (1:1,000 dilution, ab207612; Abcam), LC3-II/I (1:500 dilution, GTX100240; GeneTex), p62 (1:1,000 dilution, 5114S; CST), P-AMPK (1:500 dilution, bs-4002R; Bioss), T-AMPK (1:1,000 dilution, E-AB-33742; Elabscience), P-mTOR (1:500 dilution, bs-3494R; Bioss), T-mTOR (1:200 dilution, BM4182; Boster), PPARγ (1:500 dilution, bs-4590R; Bioss), Nuclear NF-κB (1:500 dilution, bs-0465R; Bioss), total NF-κB (1:200 dilution; Abcam), GAPDH (1:2000; Zhong Shan-Golden Bridge Biological Technology), and b-actin (1:5,000 dilution; Santa Cruz), respectively, at 4°C overnight. The western blot bands were collected by Imaging System (LI-COR Biosciences) and quantified with Odyssey v.1.2 software by measuring intensity (area × optical density [OD]) in each group with β-actin as the internal control.

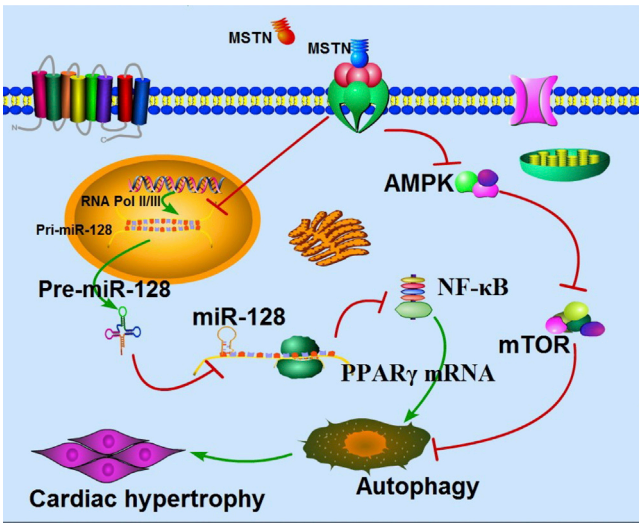

Figure 8. Schematic Diagram for the Proposed MSTN-Anti-hypertrophic Signaling Pathways

Quantitative Real-Time PCR

Total RNA from cultured neonatal rat cardiomyocytes was extracted using TRIzol reagent (Invitrogen) following the manufacturer's protocol. cDNA was synthesized by a High-Capacity cDNA Reverse Transcription Kit (Applied Biosystems). The level of miR-128 was determined using the SYBR Green I incorporation method on an ABI 7500 Fast Real-Time PCR System (Applied Biosystems), with Rnu6 (U6) as an internal control. Relative quantification of gene expression was performed with the $2^{-\Delta\Delta Ct}$ method. The sequences of primers were as follows:

miR-128, forward 5′-CGCGTCACAGTGAACCGGT-3′

reverse 5′-AGTGCAGGGTCCGAGGTATT-3′

reverse transcriptase primer: 5′-GTCGTATCCAGTGCAGGGTCC GAGGTA TTCGCACTGGATACGACAAAGAG-3′

Tandem mRFP-GFP Fluorescence Microscopy

Cells transiently expressing GFP-mRFP-LC3 were treated as designated and were then observed by laser microscopy. At least 10 cells in three independent experiments were analyzed randomly, with the investigator blinded as to the origin of each image. The number of GFP and mRFP puncta per cell was determined using Image-Pro plus 6.0. A cell was considered to be autophagic if more than 10 puncta were present in that cell.

siRNA Treatment

siRNA duplex sequences corresponding to MSTN (5′-AAGATG ACGATTATCACGCTA-3′), mTOR (5′-UGAACCCUGCCUUUG UCAUGC-3′), PPARγ (5′-AAGCCCUUCACUACUGUUGAC-3′), and a non-specific control (5′-TTCGTAAGAGACCGTGGATCC TGTC-3′) were prepared, respectively, as described by the manufacturer (Sequitur). Neonatal rat cardiomyocytes were grown in medium lacking doxycycline for 24 h and then transfected with siRNAs

(25 mmol/L) using Oligofectamine according to the manufacturer's instructions (Invitrogen).

Synthesis of miR-128 and Anti-miR-128 Antisense Inhibitors

miR-128 and antisense oligonucleotides AMO-128 were synthesized by GenePharma (Shanghai GenePharma). The sequences were as follows:

miR-128, sense 5′-UCACAGUGAACCGGUCUCUUU-3′, antisense 5′-AGAGACCGGUUCACUGUGAUU-3′

NC, sense 5′-UUCUCCGAACGUGUCACGUTT-3′, antisense 5′-ACGUGACACGUUCGGAGAATT-3′

AMO-128, 5′-AAAGAGACCGGUUCACUGUGA-3′; AMO-NC, 5′-CAGUACUUUUGUGUAGUACAA-3′

Statistical Analysis

All data were expressed as mean ± SD. Statistical analysis was performed using one-way analysis of variance followed by Bonferroni test (equal variances assumed) or Tamhane's T2 test (equal variances not assumed). Two-way ANOVA test was performed to compare significance between two distinct independent variables. Differences were considered to be statistically significant when $p < 0.05$.

SUPPLEMENTAL INFORMATION

Supplemental Information can be found online at https://doi.org/10.1016/j.omtn.2019.12.003.

AUTHOR CONTRIBUTIONS

Conceived and designed the experiments: H.S. Performed the experiments: H.Q., J.R., L.B., C.S., Q.Z., Y.C., P.S., B.F., and Y.L. Analyzed the data: H.Q. and H.S. Wrote the paper: H.Q. and H.S.

CONFLICTS OF INTEREST

The authors declare no competing interests.

ACKNOWLEDGMENTS

We thank Prof. Weidong Yong (Institute of Laboratory Animal Science, Chinese Academy of Medical Sciences, Peking Union Medical College) for generously providing the *MSTN*$^{-/-}$ rats. This project was supported by Heilongjiang Postdoctoral Foundation (LBH-Z17121) and China Postdoctoral Science Foundation (2018M630378).

REFERENCES

1. Tham, Y.K., Bernardo, B.C., Ooi, J.Y., Weeks, K.L., and McMullen, J.R. (2015). Pathophysiology of cardiac hypertrophy and heart failure: signaling pathways and novel therapeutic targets. Arch. Toxicol. *89*, 1401–1438.
2. Argilés, J.M., Orpí, M., Busquets, S., and López-Soriano, F.J. (2012). Myostatin: more than just a regulator of muscle mass. Drug Discov. Today *17*, 702–709.
3. McPherron, A.C., and Lee, S.J. (1997). Double muscling in cattle due to mutations in the myostatin gene. Proc. Natl. Acad. Sci. USA *94*, 12457–12461.
4. Rodgers, B.D., and Garikipati, D.K. (2008). Clinical, agricultural, and evolutionary biology of myostatin: a comparative review. Endocr. Rev. *29*, 513–534.
5. Allen, D.L., Cleary, A.S., Speaker, K.J., Lindsay, S.F., Uyenishi, J., Reed, J.M., Madden, M.C., and Mehan, R.S. (2008). Myostatin, activin receptor IIb, and follistatin-like-3 gene expression are altered in adipose tissue and skeletal muscle of obese mice. Am. J. Physiol. Endocrinol. Metab. *294*, E918–E927.
6. Hittel, D.S., Berggren, J.R., Shearer, J., Boyle, K., and Houmard, J.A. (2009). Increased secretion and expression of myostatin in skeletal muscle from extremely obese women. Diabetes *58*, 30–38.
7. Lin, J., Arnold, H.B., Della-Fera, M.A., Azain, M.J., Hartzell, D.L., and Baile, C.A. (2002). Myostatin knockout in mice increases myogenesis and decreases adipogenesis. Biochem. Biophys. Res. Commun. *291*, 701–706.
8. Cook, S.A., Matsui, T., Li, L., and Rosenzweig, A. (2002). Transcriptional effects of chronic Akt activation in the heart. J. Biol. Chem. *277*, 22528–22533.
9. Shyu, K.G., Lu, M.J., Wang, B.W., Sun, H.Y., and Chang, H. (2006). Myostatin expression in ventricular myocardium in a rat model of volume-overload heart failure. Eur. J. Clin. Invest. *36*, 713–719.
10. Sharma, M., Kambadur, R., Matthews, K.G., Somers, W.G., Devlin, G.P., Conaglen, J.V., Fowke, P.J., and Bass, J.J. (1999). Myostatin, a transforming growth factor-beta superfamily member, is expressed in heart muscle and is upregulated in cardiomyocytes after infarct. J. Cell. Physiol. *180*, 1–9.
11. George, I., Bish, L.T., Kamalakkannan, G., Petrilli, C.M., Oz, M.C., Naka, Y., Sweeney, H.L., and Maybaum, S. (2010). Myostatin activation in patients with advanced heart failure and after mechanical unloading. Eur. J. Heart Fail. *12*, 444–453.
12. Yang, Z., and Klionsky, D.J. (2010). Eaten alive: a history of macroautophagy. Nat. Cell Biol. *12*, 814–822.
13. Lee, K.S., Lee, M.G., Woo, Y.J., and Nam, K.S. (2019). The preventive effect of deep sea water on the development of cancerous skin cells through the induction of autophagic cell death in UVB-damaged HaCaT keratinocyte. Biomed. Pharmacother. *111*, 282–291.
14. Chung, Y., Lee, J., Jung, S., Lee, Y., Cho, J.W., and Oh, Y.J. (2018). Dysregulated autophagy contributes to caspase-dependent neuronal apoptosis. Cell Death Dis. *9*, 1189.
15. Wang, Q.Q., Zhai, C., Wahafu, A., Zhu, Y.T., Liu, Y.H., and Sun, L.Q. (2019). Salvianolic acid B inhibits the development of diabetic peripheral neuropathy by suppressing autophagy and apoptosis. J. Pharm. Pharmacol. *71*, 417–428.
16. Sagrillo-Fagundes, L., Bienvenue-Pariseault, J., and Vaillancourt, C. (2019). Melatonin: The smart molecule that differentially modulates autophagy in tumor and normal placental cells. PLoS ONE *14*, e0202458.
17. Esteves, A.R., Palma, A.M., Gomes, R., Santos, D., Silva, D.F., and Cardoso, S.M. (2019). Acetylation as a major determinant to microtubule-dependent autophagy: Relevance to Alzheimer's and Parkinson disease pathology. Biochim. Biophys. Acta. Mol. Basis Dis. *1865*, 2008–2023.
18. Lee, J.S., Kim, S.R., Song, J.H., Lee, Y.P., and Ko, H.J. (2018). Anti-human Rhinovirus 1B activity of dexamethasone via GCR-dependent autophagy activation. Osong Public Health Res. Perspect. *9*, 334–339.
19. Gottlieb, R.A., and Gustafsson, A.B. (2011). Mitochondrial turnover in the heart. Biochim. Biophys. Acta *1813*, 1295–1301.
20. Nakai, A., Yamaguchi, O., Takeda, T., Higuchi, Y., Hikoso, S., Taniike, M., Omiya, S., Mizote, I., Matsumura, Y., Asahi, M., et al. (2007). The role of autophagy in cardiomyocytes in the basal state and in response to hemodynamic stress. Nat. Med. *13*, 619–624.
21. Cao, D.J., Wang, Z.V., Battiprolu, P.K., Jiang, N., Morales, C.R., Kong, Y., Rothermel, B.A., Gillette, T.G., and Hill, J.A. (2011). Histone deacetylase (HDAC) inhibitors attenuate cardiac hypertrophy by suppressing autophagy. Proc. Natl. Acad. Sci. USA *108*, 4123–4128.
22. Zhang, X., Li, Z.L., Crane, J.A., Jordan, K.L., Pawar, A.S., Textor, S.C., Lerman, A., and Lerman, L.O. (2014). Valsartan regulates myocardial autophagy and mitochondrial turnover in experimental hypertension. Hypertension *64*, 87–93.
23. Redout, E.M., Wagner, M.J., Zuidwijk, M.J., Boer, C., Musters, R.J., van Hardeveld, C., Paulus, W.J., and Simonides, W.S. (2007). Right-ventricular failure is associated with increased mitochondrial complex II activity and production of reactive oxygen species. Cardiovasc. Res. *75*, 770–781.
24. Chen, X., Zeng, S., Zou, J., Chen, Y., Yue, Z., Gao, Y., Zhang, L., Cao, W., and Liu, P. (2014). Rapamycin attenuated cardiac hypertrophy induced by isoproterenol and maintained energy homeostasis via inhibiting NF-κB activation. Mediators Inflamm. *2014*, 868753.

25. Zeng, X.C., Li, L., Wen, H., and Bi, Q. (2016). MicroRNA-128 inhibition attenuates myocardial ischemia/reperfusion injury-induced cardiomyocyte apoptosis by the targeted activation of peroxisome proliferator-activated receptor gamma. Mol. Med. Rep. *14*, 129–136.

26. Clarke, A.J., and Simon, A.K. (2019). Autophagy in the renewal, differentiation and homeostasis of immune cells. Nat. Rev. Immunol. *19*, 170–183.

27. Ke, P.Y. (2018). The multifaceted roles of autophagy in flavivirus-host interactions. Int. J. Mol. Sci. *19*, 3940.

28. Chen, L.L., Huang, Y.J., Cui, J.T., Song, N., and Xie, J. (2019). Iron dysregulation in Parkinson's disease: focused on the autophagy-lysosome pathway. ACS Chem. Neurosci. *10*, 863–871.

29. Hooper, K.M., Barlow, P.G., Henderson, P., and Stevens, C. (2019). Interactions between autophagy and the unfolded protein response: implications for inflammatory bowel disease. Inflamm. Bowel Dis. *25*, 661–671.

30. Xu, J., Jiao, K., Liu, X., Sun, Q., Wang, K., Xu, H., Zhang, S., Wu, Y., Wu, L., Liu, D., et al. (2018). Omi/HtrA2 participates in age-related autophagic deficiency in rat liver. Aging Dis. *9*, 1031–1042.

31. Zhang, C., McFarlane, C., Lokireddy, S., Bonala, S., Ge, X., Masuda, S., Gluckman, P.D., Sharma, M., and Kambadur, R. (2011). Myostatin-deficient mice exhibit reduced insulin resistance through activating the AMP-activated protein kinase signalling pathway. Diabetologia *54*, 1491–1501.

32. Copetti, T., Bertoli, C., Dalla, E., Demarchi, F., and Schneider, C. (2009). p65/RelA modulates BECN1 transcription and autophagy. Mol. Cell. Biol. *29*, 2594–2608.

33. Johansen, T., and Lamark, T. (2011). Selective autophagy mediated by autophagic adapter proteins. Autophagy *7*, 279–296.

34. Remels, A.H., Langen, R.C., Gosker, H.R., Russell, A.P., Spaapen, F., Voncken, J.W., Schrauwen, P., and Schols, A.M. (2009). PPARgamma inhibits NF-kappaB-dependent transcriptional activation in skeletal muscle. Am. J. Physiol. Endocrinol. Metab. *297*, E174–E183.

35. Carè, A., Catalucci, D., Felicetti, F., Bonci, D., Addario, A., Gallo, P., Bang, M.L., Segnalini, P., Gu, Y., Dalton, N.D., et al. (2007). MicroRNA-133 controls cardiac hypertrophy. Nat. Med. *13*, 613–618.

36. Orenes-Piñero, E., Montoro-García, S., Patel, J.V., Valdés, M., Marín, F., and Lip, G.Y. (2013). Role of microRNAs in cardiac remodelling: new insights and future perspectives. Int. J. Cardiol. *167*, 1651–1659.

37. Gu, H., Cao, Y., Qiu, B., Zhou, Z.Q., Deng, R., Chen, Z., et al. (2016). Establishment and phenotypic analysis of an Mstn knockout rat. Biochem. Biophys. Res. Commun. *477*, 115–122.

38. Song, X.W., Li, Q., Lin, L., Wang, X.C., Li, D.F., Wang, G.K., Ren, A.J., Wang, Y.R., Qin, Y.W., Yuan, W.J., and Jing, Q. (2010). MicroRNAs are dynamically regulated in hypertrophic hearts, and miR-199a is essential for the maintenance of cell size in cardiomyocytes. J. Cell. Physiol. *225*, 437–443.

39. Yu, C.J., Tang, L.L., Liang, C., Chen, X., Song, S.Y., Ding, X.Q., Zhang, K.Y., Song, B.L., Zhao, D., Zhu, X.Y., et al. (2016). Angiotensin-converting enzyme 3 (ACE3) protects against pressure overload-induced cardiac hypertrophy. J. Am. Heart Assoc. *5*, e002680.

40. Ji, Y.X., Zhang, P., Zhang, X.J., Zhao, Y.C., Deng, K.Q., Jiang, X., Wang, P.X., Huang, Z., and Li, H. (2016). The ubiquitin E3 ligase TRAF6 exacerbates pathological cardiac hypertrophy via TAK1-dependent signalling. Nat. Commun. *7*, 11267.